Ersch. in: Molecular Biology and Evolution ; 22 (2005), 8. - S. 1635-1648
http://dx.doi.org/10.1093/molbev/msi158

Analysis of the Reticulon Gene Family Demonstrates the Absence of the Neurite Growth Inhibitor Nogo-A in Fish

Heike Diekmann,[*1] *Michael Klinger,*[*1] *Thomas Oertle,*[†‡] *Dietmar Heinz,*[*] *Hans-Martin Pogoda,*[§] *Martin E. Schwab,*[†‡] *and Claudia A. O. Stuermer*[*]

*Department of Biology, University of Konstanz, Konstanz, Germany; †Brain Research Institute, University of Zurich, Zurich, Switzerland; ‡Department of Biology, Swiss Federal Institute of Technology Zurich, Zurich, Switzerland; and §Department of Developmental Biology, Stanford University School of Medicine

Reticulons (RTNs) are a family of evolutionary conserved proteins with four RTN paralogs (RTN1, RTN2, RTN3, and RTN4) present in land vertebrates. While the exact functions of RTN1 to RTN3 are unknown, mammalian RTN4 A/Nogo A was shown to inhibit the regeneration of severed axons in the mammalian central nervous system (CNS). This inhibitory function is exerted via two distinct regions, one within the Nogo A specific N terminus and the other in the conserved reticulon homology domain (RHD). In contrast to mammals, fish are capable of CNS axon regeneration. We performed detailed analyses of the fish *rtn* gene family to determine whether this regeneration ability correlates with the absence of the neurite growth inhibitory protein Nogo A. A total of 7 *rtn* genes were identified in zebrafish, 6 in pufferfish, and 30 in eight additional fish species. Phylogenetic and syntenic relationships indicate that the identified fish *rtn* genes are orthologs of mammalian RTN1, RTN2, RTN3, and RTN4 and that several paralogous fish genes (e.g., *rtn4* and *rtn6*) resulted from genome duplication events early in actinopterygian evolution. Accordingly, sequences homologous to the conserved RTN4/Nogo RHD are present in two fish genes, *rtn4* and *rtn6*. However, sequences comparable to the first ~1,000 amino acids of mammalian Nogo A including a major neurite growth inhibitory region are absent in zebrafish. This result is in accordance with functional data showing that axon growth inhibitory molecules are less prominent in fish oligodendrocytes and CNS myelin compared to mammals.

Introduction

In the mammalian central nervous system (CNS), regeneration of severed fiber tracts is impaired by inhibitory proteins associated with CNS myelin (Filbin 2003; Schwab 2004). Nogo-A is one of the CNS myelin components that interferes with axon regrowth in the rat and mouse CNS and provokes growth cone collapse in vitro (Chen et al. 2000; GrandPré et al. 2000; Prinjha et al. 2000; Oertle et al. 2003*c*). Nogo/RTN4 is the fourth member of the reticulon (RTN) gene family that codes for proteins with a highly conserved carboxy-terminal reticulon homology domain (RHD; Pfam PF02453) and a variable amino-terminus. The RHD is 150 201 amino acids (aa) in length and is characterized by two large (>30 aa) hydrophobic stretches that are responsible for the association of RTN proteins to membranes (van de Velde et al. 1994; Oertle, Merkler, and Schwab 2003). In mammals, four RTN family members are known. RTN1 (formerly neuroendocrine specific protein NSP1), RTN2, and RTN3 are enriched in membranes of the endoplasmic reticulum (van de Velde et al. 1994), but their exact functions have not been elucidated so far. RTN4/Nogo gives rise to a number of different isoforms (Nogo-A, -B, and -C as main transcripts) both through alternative splicing and alternative promoter usage (Chen et al. 2000; Oertle et al. 2003*a*), and the largest isoform, Nogo-A/RTN4-A, is a potent neurite outgrowth inhibitor (Chen et al. 2000; GrandPré et al. 2000; Prinjha et al. 2000). In vitro assays with recombinant peptides allowed to map the inhibitory function to two different regions of the Nogo-A protein (Oertle et al. 2003*c*). One domain provoking growth cone collapse is encoded by a stretch of the Nogo-A specific exon (NiG-Δ20; aa 544 725 of rat Nogo-A; Oertle et al. 2003*c*), and antibodies against this region promote in vivo CNS regeneration in rats (Schwab 2004). The second region that induces growth cone collapse is the 66-aa loop between the two C-terminal hydrophobic domains of the RHD (Nogo-66). Nogo-66 is identical in all Nogo/RTN4 isoforms and signals through an interaction with the glycosylphosphatidylinositol-linked Nogo-66 receptor (NgR) (Fournier, GrandPré, and Strittmatter 2001; GrandPré, Li, and Strittmatter 2002).

In contrast to mammals, lesioned axons readily regenerate in the fish CNS (Gaze 1970; Stuermer 1988*a*, 1988*b*). Success of CNS axon regeneration correlates with the growth-permissive substrate properties of goldfish CNS myelin in in vitro assays (Bastmeyer et al. 1991; Wanner et al. 1995). In fact, growth cones of fish retinal axons cross fish CNS myelin but collapse when contacting mammalian CNS myelin (Bastmeyer et al. 1991). This implies that fish axons recognize neurite growth inhibitors associated with mammalian CNS myelin but that fish CNS myelin is devoid of such inhibitors (Bastmeyer et al. 1991; Wanner et al. 1995). In this context, it is an intriguing question whether Nogo-A might be the molecule causing growth cone collapse of fish axons upon contact of mammalian CNS myelin and whether Nogo-A is absent from fish myelin. Here, we show that growth of fish axons in vitro is indeed blocked by a rat Nogo-A specific peptide. To determine whether fish possess an rtn4/nogo ortholog, we cloned rtn family members. Given the high conservation in the RHD of the *rtn* gene family and the proposed fish-specific genome duplication (Taylor et al. 2003), we analyzed phylogenetic and syntenic relationships within the entire *rtn* family and unequivocally confirmed the presence of *rtn4* orthologs in fish. However, comparison of the exon composition of all fish *rtn* genes with the respective human orthologs

[1] Both authors contributed equally to this work.

Key words: *Danio rerio*, reticulon, Nogo, RTN4, gene duplication, conserved synteny.

E mail: claudia.stuermer@uni konstanz.de.

and dissection of sequence homologies within their N-termini argue for fundamental differences in the evolution of rtn1 rtn3 and rtn4: the specific N-termini of fish and mammalian rtn1, rtn2, and rtn3, respectively, evolved from a common ancestor, whereas the rtn4 N-termini must have been acquired independently. Fish RTN4 isoforms have short N-termini without any homology to mammalian Nogo-A, -B, or -C. Finally, the presence of exons homologous to the N-terminal region of mammalian Nogo-A in zebrafish was excluded by aligning the relevant genomic regions of zebrafish and human rtn4. Consequently, our results show that sequences related to the neurite growth inhibitory region of mammalian Nogo-A are absent in fish.

Materials and Methods

Axon Outgrowth Assay Using Goldfish Retinal Explants

Purified recombinant rat NiG-Δ20 peptide (aa 544 725 of rat Nogo-A; 3 mg/ml; Oertle et al. 2003*c*) was incubated as a sandwich between polylysine-coated 18 × 18-mm coverslips at 4°C overnight. The next day, coverslips were washed three times with cold modified Leibowitz medium L15 (GIBCO). Goldfish retinae were prepared 10 days after conditioning optic nerve lesion as described (Vielmetter and Stuermer 1989) and chopped into 200 × 200-μm pieces. About 50 miniexplants were plated on each NiG-Δ20 coated coverslip and incubated with F12 medium (Invitrogen, Karlsruhe, Germany) at 23°C (Wanner et al. 1995). As controls, coverslips were coated with a non-inhibitory rat Nogo-A peptide (NiG-Δ36; aa 260 415 of rat Nogo-A; 3 mg/ml; Oertle et al. 2003*c*), with a control protein (base pairs 1650 1748 of SC1, a member of the immunoglobulin superfamily, cloned into pTrcHis [Invitrogen] and purified on Ni^{2+}-NTA columns [Qiagen, Hilden, Germany] similar to NiG-Δ20), or with the buffer used for protein purification. After 20 h, the amount of explants with growing axons were counted using a phase contrast microscope (Axiovert Zeiss, Jena, Germany). A total of 1,087 miniexplants in 20 different cultures were evaluated using three independent protein purifications of the NiG-Δ20 peptide of rat Nogo-A, whereas for the SC-1 protein (3 different protein purifications) 669 miniexplants in 18 different cultures were analyzed. Significance of axon growth differences was calculated using Student's *t*-test.

Nomenclature of Fish rtn Transcripts

Zebrafish and fugu transcripts were named according to the nomenclature guidelines for RTN genes (Oertle et al. 2003*b*). In brief, *rtn* serves as a gene symbol for chordate RTNs. Paralogous rtn sequences are arbitrarily numbered. To distinguish *rtn* genes of various species, a prefix according to the identification code proposed by SWISS-PROT is used (e.g., (FUGRU)rtn4). Alternative transcripts generated by alternative promoter usage receive different letters (e.g., (FUGRU)rtn4-l, (FUGRU)rtn4-n), while alternatively spliced transcripts derived from a single promoter have the same letter but are distinguished by consecutive numbering (e.g., (FUGRU)rtn4-l1, (FUGRU)rtn4-l2).

Cloning and Sequence Analysis of Zebrafish and Fugu rtn Genes

Zebrafish and fugu *rtn* genes and transcripts were uncovered by a combination of library screening and database searches for fish expressed sequence tags (ESTs) and mRNAs with known human RTN protein sequences, reverse transcriptase polymerase chain reaction (RT-PCR), and rapid amplification of cDNA ends (RACE) (supplementary table 1A). To isolate zebrafish rtn cDNAs, two rounds of library screening were performed at the RZPD (Deutsches Ressourcenzentrum für Genomforschung GmbH, Heidelberg, Germany). The RZPD first screened high-density filters of an adult zebrafish retina library and of a late somitogenesis library using ^{33}P-labeled base pairs 2 490 of (DANRE)rtn4-n. In a subsequent approach, the same libraries plus an adult brain library were probed with ^{33}P-labeled base pairs 1739 2422 of (DANRE)rtn1-a1 and base pairs 1624 3157 of (DANRE)rtn6-a1. Obtained clones are listed in supplementary table 1A.

In addition, zebrafish and fugu cDNA and genomic sequences were obtained using Blast algorithms (Altschul et al. 1997) at the National Center for Biotechnology Information (NCBI) (www.ncbi.nlm.nih.gov/BLAST/), Ensembl (www.ensembl.org/Danio rerio/blastview and www.ensembl.org/Fugu rubripes/blastview), and the Doe Joint Genome Institute (aluminum.jgi-psf.org/prod/bin/runBlast.pl?db=fugu6) Web pages. Exon-intron structures were examined by comparing genomic sequences against cDNA sequences, respecting the GT-AG rule of splice donor and acceptor sites. For fugu *rtn* genes, without any ESTs or cDNA information available, exon sequences were deduced from the genomic sequences by comparison with the zebrafish cDNAs. In total, we uncovered 13 different zebrafish and fugu *rtn* genes with 37 mRNA variants. The sequences surrounding the putative start methionines of most fish rtn transcripts comply with the consensus motif for translation initiation (gccAcc**ATG**G) at least at one of the two most important positions (a G following the ATG and a purine at position −3; Kozak 1996). In addition, an upstream stop codon in most sequences ensures that the identified start methionines correspond to the respective N-terminus of the protein (supplementary table 1A). The predicted proteins have a more or less conserved dilysine endoplasmic reticulum membrane retention motif at their C-terminus, and the N-termini of the long splice forms (-a and -l variants) are remarkably acidic (supplementary table 1A).

We used the exon-intron information and the deduced cDNA sequences to amplify zebrafish rtn splice variants from various adult tissues (see RT-PCR) and fugu rtn transcripts from liver and brain cDNA with specific primers (supplementary tables 1A and 1B). Sequences were completed by performing 5′- and 3′-RACE, respectively. In brief, we extracted mRNA from a pool of 48-h postfertilization zebrafish embryos (FastTrack™ 2.0 kit; Invitrogen) and used 0.9 μg per reaction as template for the synthesis of either first-strand 5′-Ready cDNA using 5′-CDS and SMART II (switching mechanism at 5′end of RNA transcript) oligonucleotides or 3′-Ready cDNA using 3′-CDS primer, according to the manufacturer's instructions

(SMART RACE cDNA Amplification Kit; BD Biosciences, Erembodegem, Belgium). All polymerase chain reaction (PCR) fragments were directly subcloned into the pCRII cloning vector (Invitrogen), and plasmid DNA was prepared using the QIAprep® 8 Miniprep Kit (Qiagen). Both DNA strands were sequenced using the Abi Prism® BigDye™ Terminator Cycle Sequencing Kit (Applied Biosystems, Foster City, Calif.) and analyzed on an Abi Prism 3100 Genetic Analyzer. Single sequences were assembled using SeqMan™II of the DnaStar software package (GATC Biotech, Konstanz, Germany). Specific informations for the cloning strategy of each gene are available upon request. Sequences were deposited in GenBank and accession numbers are listed in supplementary table 1D.

Sequence Alignments and Phylogenetic Analyses

GenBank accession numbers of sequences used for the different alignments are listed in supplementary table 1D. A total of 46 partial or complete RTN mRNAs were uncovered by database searches in addition to the ones already described (Roebroek et al. 1993, 1996, 1998; Kools et al. 1994; Baka et al. 1996; Stubbs et al. 1996; Ninkina, Baka, and Buchman 1997; Geisler et al. 1998; Nagase et al. 1998; Moreira, Jaworski, and Rodriguez 1999; Morris et al. 1999; GrandPré et al. 2000; Prinjha et al. 2000; Yang et al. 2000; Hamada et al. 2002; Zhang, Harrison, and Gerstein 2002; Oertle et al. 2003*a*; Klinger et al. 2004*a*). The single *RTN* gene of the urochordate *Ciona intestinalis* was used as an out-group.

Nucleotide sequences of the RHDs were translated using BioEdit (Hall 1999) and aligned as aa using ClustalW (Thompson, Higgins, and Gibson 1994). The alignment was edited by hand and then converted back into nucleotides to produce a codon alignment that was 642 nucleotides long. Due to length variations in the *RTN2* genes, all other sequences contain a C-terminal gap of up to 60 nucleotides. Eighteen of the 86 sequences used for the analyses were incomplete either at the N- or C-terminus producing alignment gaps of different length. Phylogenies of RTN sequences were reconstructed using neighbor-joining (NJ) methods with MEGA version 2.1 (Kumar et al. 2001) and pairwise deletion of the aforementioned gaps. Support for nodes in the NJ tree was assessed using 1,000 bootstrap reiterations (Felsenstein 1985). The RHD alignment (ALIGN 000759) and similarly constructed alignments of the various rtn N-termini (ALIGN 000753, ALIGN 000754, ALIGN 000755, ALIGN 000756, ALIGN 000757, ALIGN 000758) were deposited at EMBL-ALIGN (http://www.ebi.ac.uk/embl/Submission/align top.html).

Molecular evolutionary analyses were conducted using MEGA version 2.1 (Kumar et al. 2001). In brief, sequences of the RHDs were aligned at the aa level by the ClustalW program and gaps were pairwise deleted. Numbers of nonsynonymous substitutions (aa altering) per nonsynonymous site (d_N) and synonymous substitutions (silent) per synonymous site were estimated (Nei and Gojobori 1986) for each fish paralog in separate comparisons to the respective human RTN sequence (supplementary table 1E).

Radiation Hybrid Mapping and Synteny Analysis

A conserved synteny is defined by two or more genes located on the same chromosome in fish and their orthologs located on a single chromosome in humans (Barbazuk et al. 2000). Therefore, zebrafish *rtns* were mapped on the LN54 radiation hybrid panel using standard conditions (Hukriede et al. 1999) and the respective Web interface (http://mgchd1.nichd.nih.gov:8000/zfrh/beta.cgi). Because no unequivocal result was obtained for rtn5 and rtn6 on this panel, these rtns were mapped on the Goodfellow T51 radiation hybrid panel (Research Genetics, Inc., Huntsville, Ala.) by instant mapping at http://134.174.23.167/zonrhmapper/instantMapping.htm.

For synteny analysis (Woods et al. 2000), other zebrafish genes and ESTs already mapped on the LN54 and T51 radiation hybrid panels (http://zfin.org/cgi-bin/mapper select.cgi) were assigned to putative human orthologs by BlastX searches (Altschul et al. 1997) against the NCBI human nonredundant (nr) protein sequence database (http://www.ncbi.nlm.nih.gov/blast/blast.cgi). For EST clones that have been sequenced at the 5′ and 3′ ends, both sequences were used for BlastX searches. If the results of these searches had expected scores (*E* values) of ≤ -5, the putative orthologs were further tested with reciprocal searches against the zebrafish subset of nr sequences and dbESTs. A human ortholog was confirmed if the original zebrafish gene or EST (or a gene or EST that showed highly significant overlap with the original sequence) was in the top 15 matches of the reciprocal search by TBlastN. Fugu synteny data were retrieved with MartView (http://www.ensembl.org/Fugu rubripes/martview) for all scaffolds, on which other genes could be predicted in the vicinity of the fugu *rtns*.

Percent Identity Plots of RTN4

The zebrafish clone BX324134 from nucleotides 1 to 112,195 (linkage group [LG]6), covering the entire (DANRE)*rtn4* gene, as well as the orthologous genomic sequences of the mitochondrial translation initiation factor 2 (*MTIF2*) and *RPS27A*, was aligned against 1 Mb (nucleotides 33,841,399 34,841,398) of the corresponding human region on chromosome 2p16 from the genomic contig NT 022184.13/Hs2 22340 using the minus-strand sequence. In addition, both sequences were aligned against 400 kb (nucleotides 26,300,000 26,700,000) of the orthologous mouse sequence on chromosome (Chr.) 11 from the genomic contig NT 039515.2/Mm11 39555 32 as previously described in Oertle et al. (2003*a*). Using a newly generated exon mask for the human genes *MTIF2*, *RPS27A*, *FLJ31438*, and *RTN4* and a mask for repetitive sequences using the RepeatMasker software (http://repeatmasker.org), the percent identity plots (PIPs) were generated using MultiPipMaker (http://bio.cse.psu.edu/cgi-bin/multipipmaker) and the dot plot was generated using Advanced PipMaker (http://bio.cse.psu.edu/cgi-bin/pipmaker?advanced) according to the published method (Schwartz et al. 2000). The output was modified as in Oertle et al. (2003*a*). The same procedure was adopted using the mVista Software (http://genome.lbl.gov/vista.index.shtml) according

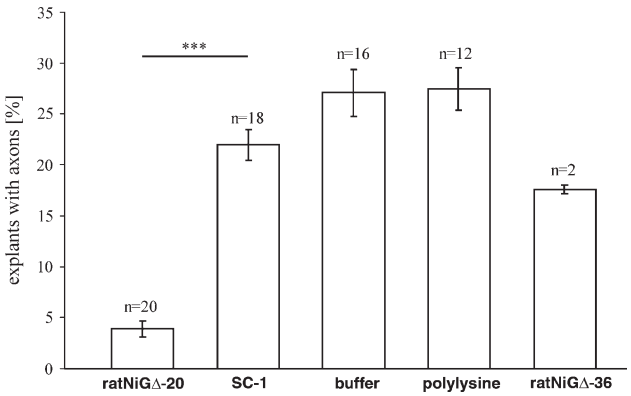

FIG. 1. Axon outgrowth assay. Percentage of goldfish retinal mini explants with axons grown after 20 h in culture. Axon growth on rat control protein SC 1, elution buffer, and polylysine treated coverslips was robust and about six times higher than that on the NiG Δ20 peptide of rat Nogo A. Moreover, a similar result was obtained in a separate experiment using NiG Δ36 of rat Nogo A as control peptide. Bars in each column represent standard error, and asterisks indicate significant difference ($P < 0.001$) by Student's t test.

to the published methodology (Mayor et al. 2000) with comparable results to the plots generated by PipMaker.

Reverse Transcriptase Polymerase Chain Reaction

A total of 100 zebrafish embryos (approximately 100 mg) for each stage or 50 mg of various adult tissues were used for the preparation of total RNA with the RNeasy Mini Prep Kit (Qiagen) following manufacturer's instructions. Muscle tissue was additionally subjected to proteinase K digestion (200 μg per 30 mg tissue). First-strand cDNA was synthesized under standard conditions with the Superscript First-Strand Synthesis System (Invitrogen) using oligo(dT)$_{12–18}$ primer. Zero transcriptions (without Superscript II in the reaction) were performed in parallel to control for genomic DNA contaminations in subsequent PCRs. Amount and quality of the different cDNA samples were evaluated comparing the expression level of the housekeeping gene actin. Informations on primer sequences and PCR conditions are listed in supplementary tables 1B and 1C.

Results

Growth Inhibition of Fish Axons by Rat Nogo-A

Goldfish retinal axons are able to regenerate and grow over isolated fish oligodendrocytes in vitro. In contrast, growth of fish axons is inhibited by rat oligodendrocytes (Bastmeyer et al. 1991; Wanner et al. 1995). To determine whether this inhibition might be mediated by Nogo-A protein, we evaluated growth of fish axons on the most inhibitory fragment of rat Nogo-A (NiG-Δ20; aa 544 725; Oertle et al. 2003*c*). Number of retinal explants with axons on recombinantly expressed Nogo-A peptide (NiG-Δ20) was compared to growth on noninhibitory Nogo-A peptide (NiG-Δ36; aa 260 415; Oertle et al. 2003*c*), unrelated control protein (SC-1), purification buffer, and polylysine (fig. 1). After 20 h in culture, explants with axons on Nogo-A NiG-Δ20 coated coverslips were rare (4%), as opposed to 18% explants with axons on NiG-Δ36 peptide, 22% on control protein (SC-1), 27% on buffer, and 27.5% on polylysine-coated coverslips. This growth inhibition on purified Nogo-A NiG-Δ20 peptide is comparable to that seen on rat CNS myelin (Wanner et al. 1995) and convincingly demonstrated a strong influence of rat Nogo-A on the growth of goldfish retinal axons. An intriguing question now is whether the capacity of fish to regenerate lesioned axons correlates with the absence of Nogo-A.

Identification of Fish rtns and Their Phylogenetic Relationships

To determine whether or not true rtn4 orthologs exist in fish, we classified newly identified fish rtns by phylogenetic analysis of the vertebrate *RTN* gene family. Characterization of all fish *rtn* family members avoided conceivable misidentification due to high conservation of the RHD and ensured the detection of paralogous *rtn* genes resulting from the proposed fish-specific genome duplication. We physically cloned seven *rtn* family members from zebrafish (*Danio rerio*) and five from pufferfish (*Takifugu rubripes*) by library screening, RT-PCR, and RACE (supplementary table 1A). Database searches uncovered a sixth *rtn* gene within the fugu genome and 46 new partial or complete vertebrate RTN mRNAs (supplementary table 1D) compared to the ones already described (Oertle et al. 2003*b*). We produced an unambiguous alignment of all 86 vertebrate RTN sequences, representing the conserved RHD (ALIGN 000759). Phylogenetic reconstruction produced a tree comprising distinct, well-supported RTN1, RTN2, RTN3, and RTN4 clades (fig. 2). Each clade included human, mouse, rat, and several other tetrapod sequences; at least one zebrafish and one fugu sequence; and a variable number of other fish species, indicating that gene duplication events producing RTN1, RTN2, RTN3, and RTN4 occurred before the divergence of ray-finned fish (actinopterygians) and tetrapods (sarcopterygians). The assignment of four distinct RTN clades was supported by the identification of aa residues unique to one subfamily of *rtn* genes (supplementary fig. 1). The RTN1 and RTN2 subfamilies are each defined by two unique and derived (not ancestral) aa substitutions. RTN3 proteins have one diagnostic and derived residue, whereas no diagnostic residues could be identified for the RTN4 subfamily (supplementary fig. 1).

All clades except RTN3 contained two zebrafish genes and the RTN2 and RTN3 clades included two fugu genes (fig. 2). Consequently, the zebrafish and fugu genes were named (DANRE)*rtn1 rtn4* and (FUGRU)*rtn1 rtn4*, respectively, and additional fish genes were consecutively numbered according to the nomenclature guidelines for RTN genes (Oertle et al. 2003*b*), i.e., (DANRE)*rtn5*, *rtn6*, and *rtn8*, and (FUGRU)*rtn7* and *rtn8*. Fish sequences within one clade did not cluster according to species but subdivided into two subclades, each containing one of the duplicated zebrafish and/or fugu genes (fig. 2). The relationships in the resulting subclades are similar, e.g., the zebrafish genes are closely related to carp ((CYPCA)*rtn1*, *3*, *4*, *5*, *6*) and goldfish ((CARAU)*rtn3*, *4*) and fugu

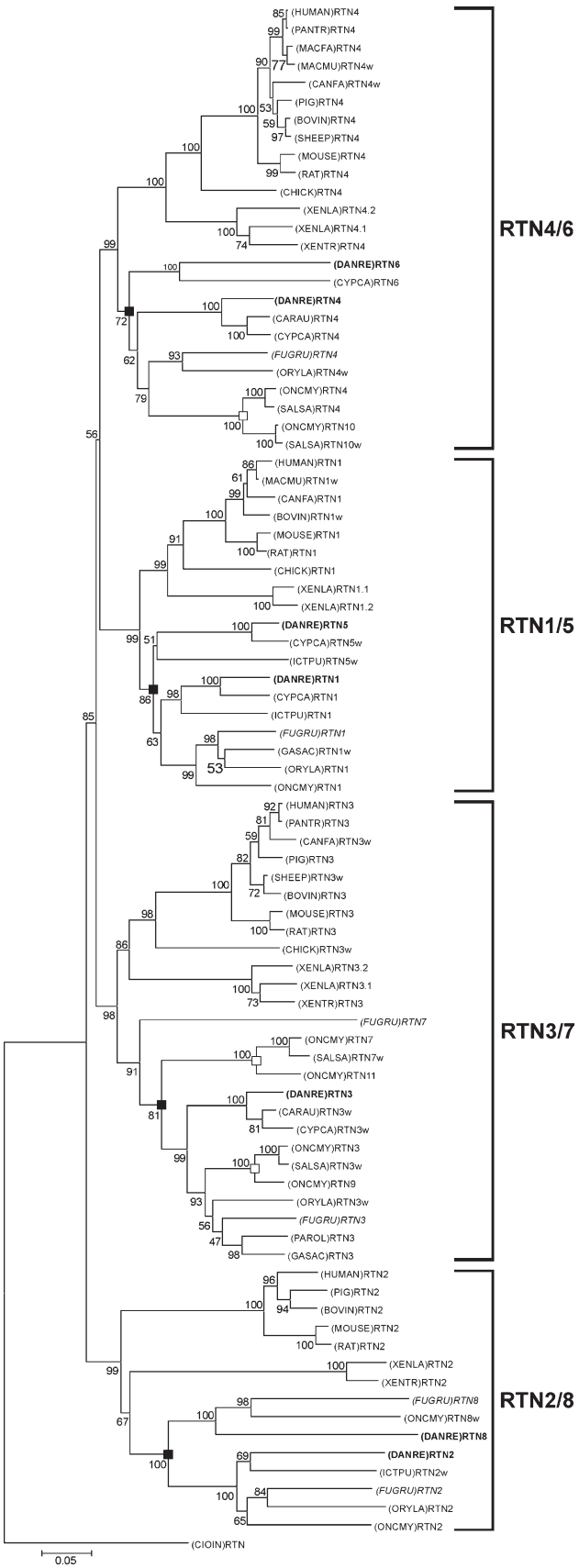

genes are closely related to medaka ((ORYLA)*rtn2*, *3*, *4*, *8*). This topology is consistent with the hypothesis that the duplicates of *rtn1 rtn4* were produced before the ancestors of zebrafish and fugu diverged. The relationships between the 13 trout and salmon sequences included in this study argue for an additional Salmonidae-specific genome duplication.

To examine whether one of the two zebrafish or fugu paralogs ((DANRE)*rtn1*/*5*, *rtn2*/*8*, *rtn4*/*6* and (FUGRU)*rtn2*/*8*, *rtn3*/*7*) evolved faster and is therefore more distantly related to the respective human RTN, we calculated the rates of synonymous (silent) and nonsynonymous (aa altering) nucleotide substitutions (d_S and d_N; Nei and Gojobori 1986). All zebrafish and fugu *rtns* accumulated similar numbers of silent nucleotide changes, but aa-altering substitutions were retained to a different extent (supplementary table 1E). In particular, twice as many changes were fixed in zebrafish *rtn6* compared to *rtn4*, indicating that the *rtn6* duplicate has evolved faster and is therefore more distantly related to human RTN4.

Taken together, our phylogenetic analysis served to assign the identified fish genes to the correct RTN subfamily and provided evidence for the existence of orthologous *rtn*4 genes in fish. In addition, we found duplications for all mammalian RTN tetralogs in zebrafish (*rtn1*/*5*, *rtn2*/*8*, *rtn4*/*6*) and/or in fugu (*rtn2*/*8*, *rtn3*/*7*), resulting in two paralogous genes in the respective species.

Conserved Syntenies of Fish and Human rtns

To unequivocally confirm the identity of the fish *rtn* genes by a second nonbioinformatical method, syntenic relationships were analyzed. Zebrafish *rtn1*, *rtn2*, *rtn3*, *rtn4*, and *rtn8* were mapped on LG20, LG15, LG7, LG6, and LG21, respectively. Both *rtn5* and *rtn6* lie on LG13. The chromosomal positions of the mapped zebrafish *rtn* genes were then compared to the locations of human RTNs (fig. 3, supplementary table 1F K).

(DANRE)*rtn1* together with 15 additional ESTs and the genes *e(r)* and *esr2a* on LG20 and (DANRE)*rtn5* with 10 ESTs on LG13 both extend existing syntenies within the same region (14q22 14q33) of human Chr. 14 (fig. 3*A* and *B*; Woods et al. 2000). This indicates that zebrafish *rtn1* and *rtn5* result from a fish-specific duplication of this

←

FIG. 2. Evolutionary relationships among vertebrate RTN genes. Phylogenetic relationships of vertebrate RTN sequences as determined by NJ method with 1,000 bootstrap reiterations based on a 642 bp long alignment of the RHDs (ALIGN 000759). *Ciona intestinalis* was used as an out group. Nodes that reflect genome duplication early during fish evolution and nodes that reflect the salmonid genome duplication are highlighted with filled and open boxes, respectively. Zebrafish and fugu sequences are written in bold and italics, respectively. Sequences that did not comprise the full RHD received the suffix "w." The scale represents 5% nucleotide sequence divergence. Abbreviations: BOVIN, *Bos taurus*; CANFA, *Canis familiaris*; CARAU, *Carassius auratus*; CHICK, *Gallus gallus*; CIOIN, *Ciona intestinalis*; CYPCA, *Cyprinus carpio*; DANRE, *Danio rerio*; FUGRU, *Takifugu rubripres*; GASAC, *Gasterosteus aculeatus*; ICTPU, *Ictalurus punctatus*; HUMAN, *Homo sapiens*; MACMU, *Macaca mulatta*; MACFA, *Macaca fascicularis*; MOUSE, *Mus musculus*; ONCMY, *Oncorhynchus mykiss*; ORYLA, *Oryzias latipes*; PANTR, *Pan troglodytes*; PAROL, *Paralichthys olivaceus*; PIG, *Sus scrofa*; RAT, *Rattus norvegicus*; SHEEP, *Ovis aries*; SALSA, *Salmo salar*; XENLA, *Xenopus laevis*; XENTR, *Silurana tropicalis*.

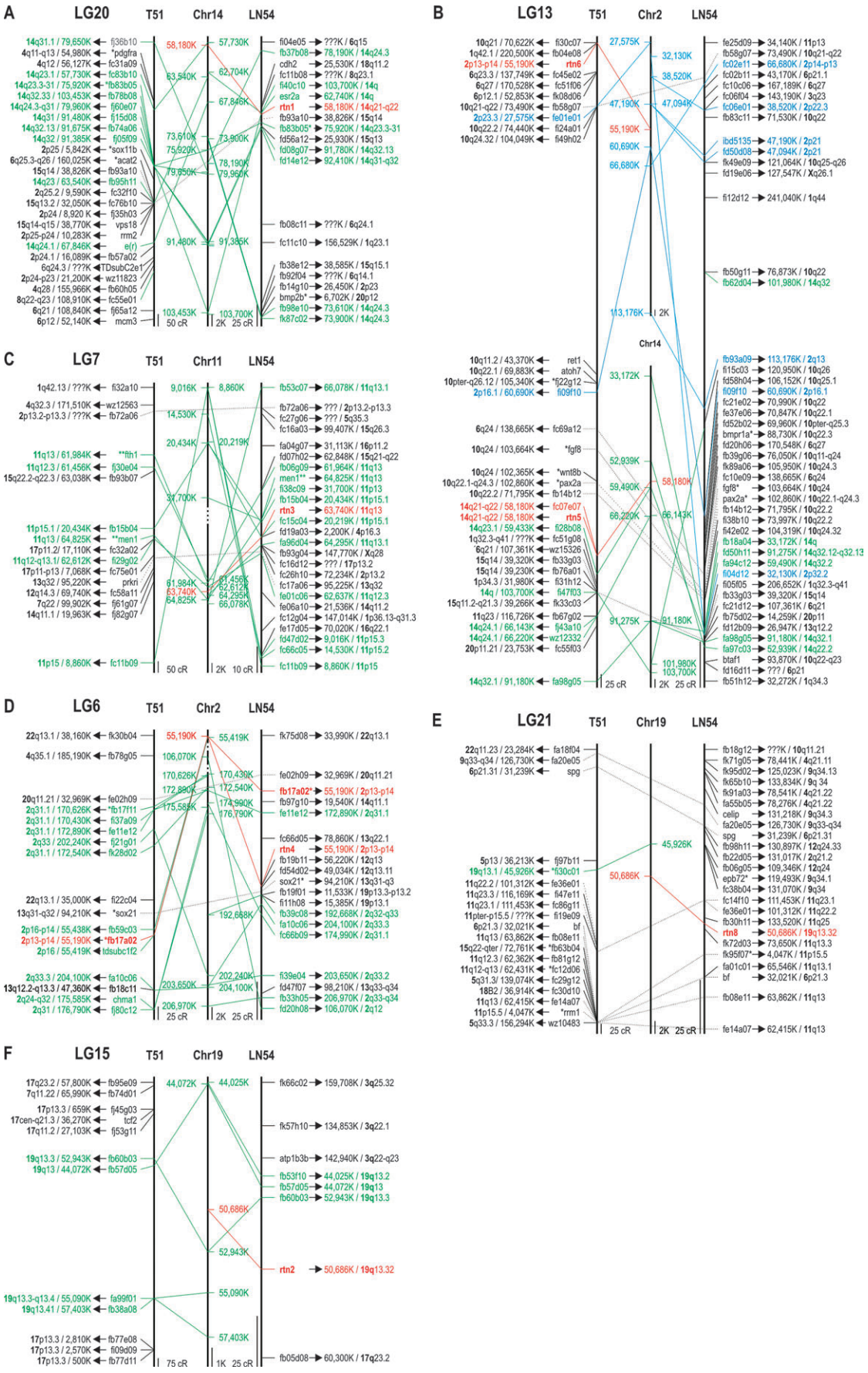
A
LG20
T51
Chr14
LN54
14q31.1 / 79,650K ← fj36b10
4q11-q13 / 54,980K ← *pdgfra
4q12 / 56,127K ← fc31a09
14q23.1 / 57,730K ← fc83b10
14q23.3-31 / 75,920K ← *fb83b05
14q32.33 / 103,453K ← fb78b08
14q24.3-q31 / 79,960K ← fj60e07
14q31 / 91,480K ← fj15d08
14q32.13 / 91,675K ← fb74a06
14q32 / 91,385K ← fj05f09
2p25 / 5,842K ← *sox11b
6q25.3-q26 / 160,025K ← *acat2
15q14 / 38,826K ← fb93a10
14q23 / 63,540K ← fb95h11
2q25.2 / 9,590K ← fc32f10
15q13.2 / 32,050K ← fc76b10
2p24 / 8,920 K ← fj35h03
15q14-q15 / 38,770K ← vps18
2p25-p24 / 10,283K ← rrm2
14q24.1 / 67,846K ← e(r)
2p24.1 / 16,089K ← fb57a02
6q24.3 / ???K ← TDsubC2e1
2p24-p23 / 21,200K ← wz11823
4q28 / 155,966K ← fb60h05
8q22-q23 / 108,910K ← fc55e01
6q21 / 108,840K ← fj65a12
6p12 / 52,140K ← mcm3
58,180K
63,540K
73,610K
75,920K
79,650K
91,480K
103,453K
50 cR
57,730K
62,704K
67,846K
73,900K
78,190K
79,960K
91,385K
103,700K
2K 25 cR
fi04e05 → ???K / 6q15
fb37b08 → 78,190K / 14q24.3
cdh2 → 25,530K / 18q11.2
fc11b08 → ???K / 8q23.1
fi40c10 → 103,700K / 14q
esr2a → 62,740K / 14q
rtn1 → 58,180K / 14q21-q22
fb93a10 → 38,826K / 15q14
fb83b05* → 75,920K / 14q23.3-31
fd56a12 → 25,930K / 15q13
fd08g07 → 91,780K / 14q32.13
fd14e12 → 92,410K / 14q31-q32
fb08c11 → ???K / 6q24.1
fc11c10 → 156,529K / 1q23.1
fb38e12 → 38,585K / 15q15.1
fb92f04 → ???K / 6q14.1
fb14g10 → 26,450K / 2p23
bmp2b* → 6,702K / 20p12
fb98e10 → 73,610K / 14q24.3
fk87c02 → 73,900K / 14q24.3
B
LG13
T51
Chr2
LN54
10q21 / 70,622K ← fi30c07
1q42.1 / 220,500K ← fb04e08
2p13-p14 / 55,190K ← rtn6
6q23.3 / 137,749K ← fc45e02
6q27 / 170,528K ← fc51f06
6p12.1 / 52,853K ← fk08d06
10q21-q22 / 73,490K ← fb58g07
2p23.3 / 27,575K ← fe01e01
10q22.2 / 74,440K ← fi24a01
10q24.32 / 104,049K ← fi49h02
27,575K
47,190K
55,190K
60,690K
66,680K
113,176K
32,130K
38,520K
47,094K
2K
Chr14
fe25d09 → 34,140K / 11p13
fb58g07 → 73,490K / 10q21-q22
fc02e11 → 66,680K / 2p14-p13
fc02b11 → 43,170K / 6p21.1
fc10c06 → 167,189K / 6q27
fc06f04 → 143,190K / 3q23
fc06e01 → 38,520K / 2p22.3
fb83c11 → 71,530K / 10q22
ibd5135 → 47,190K / 2p21
fd50d08 → 47,094K / 2p21
fk49e09 → 121,064K / 10q25-q26
fd19e06 → 127,547K / Xq26.1
fi12d12 → 241,040K / 1q44
fb50g11 → 76,873K / 10q22
fb62d04 → 101,980K / 14q32
10q11.2 / 43,370K ← ret1
10q22.1 / 69,883K ← atoh7
10pter-q26.12 / 105,340K ← *fj22g12
2p16.1 / 60,690K ← fi09f10
6q24 / 138,665K ← fc69a12
10q24 / 103,664K ← *fgf8
10q24 / 102,365K ← *wnt8b
10q22.1-q24.3 / 102,860K ← *pax2a
10q22.2 / 71,795K ← fb14b12
14q21-q22 / 58,180K ← fc07e07
14q21-q22 / 58,180K ← rtn5
14q23.1 / 59,433K ← fi28b08
1q32.3-q41 / ???K ← fc51g08
6q21 / 107,361K ← wz15326
15q14 / 39,320K ← fb33g03
15q14 / 39,230K ← fb76a01
1p34.3 / 31,980K ← fi31h12
14q / 103,700K ← fi47f03
15q11.2-q21.3 / 39,266K ← fk33c03
11q23 / 116,726K ← fb67g02
14q24.1 / 66,143K ← fj43a10
14q24.1 / 66,220K ← wz12332
20p11.21 / 23,753K ← fc55f03
14q32.1 / 91,180K ← fa98g05
33,172K
52,939K
58,180K
59,490K
66,220K
66,143K
91,275K
91,180K
101,980K
103,700K
25 cR
2K 25 cR
fb93a09 → 113,176K / 2q13
fi15c03 → 120,950K / 10q26
fd58h04 → 106,152K / 10q25.1
fi09f10 → 60,690K / 2p16.1
fc21e02 → 70,990K / 10q22
fe37e06 → 70,847K / 10q22.1
fd52b02 → 69,960K / 10pter-q25.3
bmpr1a* → 88,730K / 10q22.3
fd20h06 → 170,548K / 6q27
fb39g06 → 76,050K / 10q11-q24
fk89a06 → 105,950K / 10q24.3
fc10e09 → 138,665K / 6q24
fgf8* → 103,664K / 10q24
pax2a* → 102,860K / 10q22.1-q24.3
fb14b12 → 71,795K / 10q22.2
fi38b10 → 73,997K / 10q22.2
fi42e02 → 104,319K / 10q24.32
fb18a04 → 33,172K / 14q
fd50h11 → 91,275K / 14q32.12-q32.13
fa94c12 → 59,490K / 14q32.2
fi04d12 → 32,130K / 2p32.2
fi05f05 → 206,652K / 1q32.3-q41
fb33g03 → 39,320K / 15q14
fc21d12 → 107,361K / 6q21
fb75d02 → 14,259K / 20p11
fd12b09 → 26,947K / 13q12.2
fa98g05 → 91,180K / 14q32.1
fa97c03 → 52,939K / 14q22.2
btaf1 → 93,870K / 10q22-q23
fd16d11 → ??? / 6p21
fb51h12 → 32,272K / 1q34.3
C
LG7
T51
Chr11
LN54
1q42.13 / ???K ← fi32a10
4q32.3 / 171,510K ← wz12563
2p13.2-p13.3 / ???K ← fb72a06
11q13 / 61,984K ← **fth1
11q12.3 / 61,456K ← fj30e04
15q22.2-q22.3 / 63,038K ← fb93b07
11p15.1 / 20,434K ← fb15b04
11q13 / 64,825K ← **men1
17p11.2/ 17,110K ← fc32a02
11q12-q13.1/ 62,612K ← fi29g02
17p11-p13 / 7,068K ← fc75e01
13q32 / 95,220K ← prkri
12q14.3 / 69,740K ← fc58a11
7q22 / 99,902K ← fj61g07
14q11.1 / 19,963K ← fj82g07
11p15 / 8,860K ← fc11b09
9,016K
14,530K
20,434K
31,700K
61,984K
63,740K
64,825K
50 cR
8,860K
20,219K
61,456K
62,612K
64,295K
66,078K
2K 10 cR
fb53c07 → 66,078K / 11q13.1
fb72a06 → ??? / 2p13.2-p13.3
fc27g06 → ??? / 5q35.3
fc16a03 → 99,407K / 15q26.3
fa04g07 → 31,113K / 16p11.2
fd07h02 → 62,848K / 15q21-q22
fb06g09 → 61,964K / 11q13
men1** → 64,825K / 11q13
fi38c09 → 31,700K / 11p13
fb15b04 → 20,434K / 11p15.1
rtn3 → 63,740K / 11q13
fc15c04 → 20,219K / 11p15.1
fd19a03 → 2,200K / 4p16.3
fa96d04 → 64,295K / 11q13.1
fb93g04 → 147,770K / Xq28
fc16d12 → ??? / 17p13.2
fc26h10 → 72,234K / 2p13.2
fc17a06 → 95,225K / 13q32
fe01c06 → 62,637K / 11q12.3
fe06a10 → 21,536K / 14q11.2
fc12g04 → 147,014K / 1p36.13-q31.3
fe17d05 → 70,020K / 16q22.1
fd47d02 → 9,016K / 11p15.3
fc66c05 → 14,530K / 11p15.2
fc11b09 → 8,860K / 11p15
D
LG6
T51
Chr2
LN54
22q13.1 / 38,160K ← fk30b04
4q35.1 / 185,190K ← fb78g05
20q11.21 / 32,969K ← fe02h09
2q31.1 / 170,626K ← *fb17f11
2q31.1 / 170,430K ← fi37a09
2q31.1 / 172,890K ← fe11e12
2q33 / 202,240K ← fj21g01
2q31.1 / 172,540K ← fk28d02
22q13.1 / 35,000K ← fi22c04
13q31-q32 / 94,210K ← *sox21
2p16-p14 / 55,438K ← fb59c03
2p13-p14 / 55,190K ← *fb17a02
2p16 / 55,419K ← tdsubc1f2
2q33.3 / 204,100K ← fa10c06
13q12.2-q13.3 / 47,360K ← fb18c11
2q24-q32 / 175,585K ← chma1
2q31 / 176,790K ← fj80c12
55,190K
106,070K
170,626K
172,880K
175,588K
203,650K
206,970K
25 cR
55,419K
170,430K
172,540K
174,990K
176,790K
192,668K
202,240K
204,100K
2K 25 cR
fk75d08 → 33,990K / 22q13.1
fe02h09 → 32,969K / 20q11.21
fb17a02* → 55,190K / 2p13-p14
fb97g10 → 19,540K / 14q11.1
fe11e12 → 172,890K / 2q31.1
fc66d05 → 78,860K / 13q22.1
rtn4 → 55,190K / 2p13-p14
fb19b11 → 56,220K / 12q13
fd54d02 → 49,034K / 12q13.11
sox21* → 94,210K / 13q31-q3
fb19f01 → 11,533K / 19p13.3-p13.2
fi11h08 → 15,385K / 19p13.1
fb39c08 → 192,668K / 2q32-q33
fa10c06 → 204,100K / 2q33.3
fc66b09 → 174,990K / 2q31.1
fi39e04 → 203,650K / 2q33.2
fd47f07 → 98,210K / 13q33-q34
fb33h05 → 206,970K / 2q33-q34
fd20h08 → 106,070K / 2q12
E
LG21
T51
Chr19
LN54
22q11.23 / 23,284K ← fa18f04
9q33-q34 / 126,730K ← fa20e05
6p21.31 / 31,239K ← spg
5p13 / 36,213K ← fj97b11
19q13.1 / 45,926K ← *fi30c01
11q22.2 / 101,312K ← fe36e01
11q23.3 / 116,169K ← fi47e11
11q23.1 / 111,453K ← fc86g11
11pter-p15.5 / ???K ← fi19e09
6p21.3 / 32,021K ← bf
11q13 / 63,862K ← fb08e11
15q22-qter / 72,761K ← *fb63b04
11q12.3 / 62,362K ← fb81g12
11q12-q13 / 62,431K ← *fc12d06
5q31.3/ 139,074K ← fc29g12
18B2 / 36,914K ← fc30d10
11q13 / 62,415K ← fe14a07
11p15.5 / 4,047K ← *rrm1
5q33.3 / 156,294K ← wz10483
45,926K
50,686K
25 cR
2K 25 cR
fb18g12 → ???K / 10q11.21
fk71g05 → 78,441K / 4q21.11
fk95d02 → 125,023K / 9q34.13
fk65b10 → 133,834K / 9q 34
fk91a03 → 78,541K / 4q21.22
fa55b05 → 78,276K / 4q21.22
celip → 131,218K / 9q34.3
fa20e05 → 126,730K / 9q33-q34
spg → 31,239K / 6p21.31
fb98h11 → 130,897K / 12q24.33
fb22d05 → 131,017K / 2q21.2
fb06g05 → 109,346K / 12q24
epb72* → 119,493K / 9q34.1
fc38b04 → 131,070K / 9q34
fc14f10 → 111,453K / 11q23.1
fe36e01 → 101,312K / 11q22.2
fb30h11 → 133,520K / 11q25
rtn8 → 50,686K / 19q13.32
fk72d03 → 73,650K / 11q13.3
fk95f07* → 4,047K / 11p15.5
fa01c01 → 65,546K / 11q13.1
bf → 32,021K / 6p21.3
fb08e11 → 63,862K / 11q13
fe14a07 → 62,415K / 11q13
F
LG15
T51
Chr19
LN54
17q23.2 / 57,800K ← fb95e09
7q11.22 / 65,990K ← fb74d01
17p13.3 / 659K ← fj45g03
17cen-q21.3 / 36,270K ← tcf2
17q11.2 / 27,103K ← fj53g11
19q13.3 / 52,943K ← fb60b03
19q13 / 44,072K ← fb57d05
19q13.3-q13.4 / 55,090K ← fa99f01
19q13.41 / 57,403K ← fb38a08
17p13.3 / 2,810K ← fb77e08
17p13.3 / 2,570K ← fi09d09
17p13.3 / 500K ← fb77d11
44,072K
50,686K
52,943K
55,090K
57,403K
75 cR
44,025K
fk66c02 → 159,708K / 3q25.32
fk57h10 → 134,853K / 3q22.1
atp1b3b → 142,940K / 3q22-q23
fb53f10 → 44,025K / 19q13.2
fb57d05 → 44,072K / 19q13
fb60b03 → 52,943K / 19q13.3
rtn2 → 50,686K / 19q13.32
1K 25 cR
fb05d08 → 60,300K / 17q23.2

segment and are therefore both orthologous to human RTN1. (DANRE)*rtn2* together with five ESTs (fig. 3*F*) and (DANRE)*rtn8* together with EST fi30c01 (fig. 3*E*) both define the so far unrecognized small syntenic groups with the region around RTN2 on human Chr. 19. Mapping of (DANRE)*rtn3*, *12* additional ESTs, and the 2 genes *fth1* and *men1* confirmed the large syntenic region between zebrafish LG7 and human Chr. 11 (fig. 3*C*; Yoder and Litman 2000). (DANRE)*rtn4* belongs to a known syntenic group on zebrafish LG6 and human Chr. 2 (Woods et al. 2000; fig. 3*D*), supported by 15 additional ESTs and the gene *chma1*. (DANRE)*rtn6* and eight other ESTs on LG13 are also syntenic to human Chr. 2 (fig. 3*B*), providing additional evidence that (DANRE)*rtn6* resulted from a fish-specific duplication and is therefore a second ortholog of human RTN4.

The six fugu *rtn* genes were identified within the genomic sequences of scaffolds 188 (rtn1), 257 (rtn2), 346 (rtn3), 2616 (rtn4), 2117 (rtn8), 3887 (rtn7, all scaffolds Ensembl release 19.2.1), and 6658 (rtn7, NCBI). Predicted genes in the vicinity of the fugu *rtns* were compared with the chromosomal localization of their respective mammalian ortholog. Again conserved syntenies were revealed for genes near *rtn1* and human Chr. 14, for *rtn2* and human Chr. 19, and for *rtn3* and human Chr. 11 (supplementary table 1L).

Summarizing, the comparative mapping results in both species support the phylogenetic classification of fish *rtns* into four RTN subfamilies (RTN1, RTN2, RTN3, and RTN4) and the fish-specific duplications leading to *rtn5*, *rtn8*, *rtn7*, and *rtn6*. Both methods emphasize that two zebrafish orthologs of human RTN4 have been identified.

Nonhomogeneous Evolution of rtn Genes

Having ascertained the presence of orthologous *rtn4* genes in fish (based on the conserved RHD), we determined the genomic organization and the N-terminal sequences of all fish *rtn* genes in comparison to the respective human orthologs to analyze the evolution of the variable N-termini and to examine whether domains homologous to the growth inhibitory regions in the N-terminus of mammalian Nogo-A (i.e., NiG-Δ20) are present in fish.

Zebrafish *rtn1* and *rtn5* are formed by at least 10 exons that can give rise to several isoforms (rtn1-a, rtn1-c and rtn5-a, rtn5-c, respectively) by alternative promoter usage (fig. 4*A*). For rtn1-a and rtn5-a, two splice forms each were detected, either with (-a1) or without (-a2) exons II + III. Cryptic splicing generated additional rtn5-a1 variants (supplementary fig. 2*C*). In the fugu genome, the one *rtn1* ortholog comprises nine exons coding for the -a isoform (fig. 4*A*).

Rtn2 is the most divergent of the RTN tetralogs with a longer RHD due to nucleotide insertions in the last exon. We found two paralogs each in zebrafish and fugu (*rtn2* and *rtn8*). Based on sequence analyses, one could speculate that the insertions present in mammalian RTN2 (36 or 39 bp) and fish *rtn2/8* (33 66 bp) occurred independently (ALIGN 000759). All identified fish *rtn2* and *rtn8* genes are built by at least seven exons, and the resulting transcripts (zebrafish and fugu rtn2-c and rtn8-c) bear only a short specific N-terminus of four aa in both species (fig. 4*B*, ALIGN 000755).

The eight exons of (DANRE)*rtn3* can give rise to two different splice variants (fig. 4*C*), encompassing either all exons (rtn3-a2) or lacking exon II (rtn3-a1). In fugu, only the rtn3-a1 transcript was found (fig. 4*C*). The sequence of the second paralog, (FUGRU)rtn7, was deduced from genomic scaffolds because no transcripts could be found in databases or amplified from liver and brain cDNA. Therefore, we cannot exclude the possibility that it represents a nontranscribed pseudogene. Interestingly, (FUGRU)*rtn7* is the only vertebrate RTN identified so far, in which the first exon of the RHD is subdivided by an extra intron (fig. 4*C*).

Rtn4 is formed by at least nine exons in zebrafish and eight exons in fugu. In zebrafish, three different mRNAs (rtn4-l, -m, and -n) are generated by alternative promoter usage, each consisting of one specific exon and the RHD with six exons (fig. 4*D*). From fugu cDNA, only the -l and -n transcripts were isolated. Fugu rtn4-l differs by the presence of two additive small exons (fig. 4*D*), leading to three splice variants (rtn4-l1, -l2, and -l3). The second zebrafish rtn4 ortholog, (DANRE)*rtn6*, comprises nine exons, and three alternative splice forms (rtn6-a1, -a2, and -a3) are produced by inclusion or exclusion of exon II or exon III (fig. 4*D*). Several other zebrafish rtn4 and rtn6 mRNA variants spliced at cryptic donor and acceptor sites were detected by RT-PCR (supplementary fig. 2*A* and *B*).

These extensive analyses of the genomic organization revealed that all identified zebrafish and fugu *rtn* genes share the same exon-intron structure in the C-terminal RHD (fig. 4, supplementary table 2), which is also conserved in mammals and reflects the high degree of sequence similarity in this region (ALIGN 0007591). The RHDs are each encoded by six exons of identical sizes (208, 139, 70, 47, 59, and 40/43/49 bp), except for *rtn2* orthologs which have a longer last exon and for (FUGRU)*rtn7* which has an additional intron in the first RHD exon. Intron phases between the RHD-encoding exons show a consistent pattern

←

FIG. 3. Analyses of zebrafish and human syntenic relationships. Map locations of ESTs and genes in the radiation hybrid panels T51 and LN54 were obtained from zebrafish information network (ZFIN). The relative chromosomal locations of the human orthologs were deduced from data in LocusLink. Markers that are syntenic to rtn1, rtn3, rtn4, and rtn5 (red) are shown in green. ESTs supporting a synteny of rtn6 and human Chr. 2 are shown in blue. Markers present on more than one zebrafish panel are connected by dotted lines. (*A*) Conserved synteny of zebrafish LG20 and human Chr. 14 defined by (DANRE)rtn1 (red). (*B*) Conserved synteny of zebrafish LG13 and human Chr. 14 defined by (DANRE)rtn5 (red) and conserved synteny of zebrafish LG13 and human Chr. 2 defined by (DANRE)rtn6 (red). (*C*) Conserved synteny of zebrafish LG7 and human Chr. 11 defined by (DANRE)rtn3 (red). (*D*) Conserved synteny of zebrafish LG6 and human Chr. 2 defined by (DANRE)rtn4 (red). (*E*) Conserved synteny of zebrafish LG21 and human Chr. 19 defined by (DANRE)rtn8 (red). (*F*) Conserved synteny of zebrafish LG15 and human Chr. 19 defined by (DANRE)rtn2 (red). Abbreviations: cR, centiray; K, kilobasepairs; *, EST and genes have been published by (Woods et al. 2000); **, EST and genes have been published by Yoder and Litman (2000).

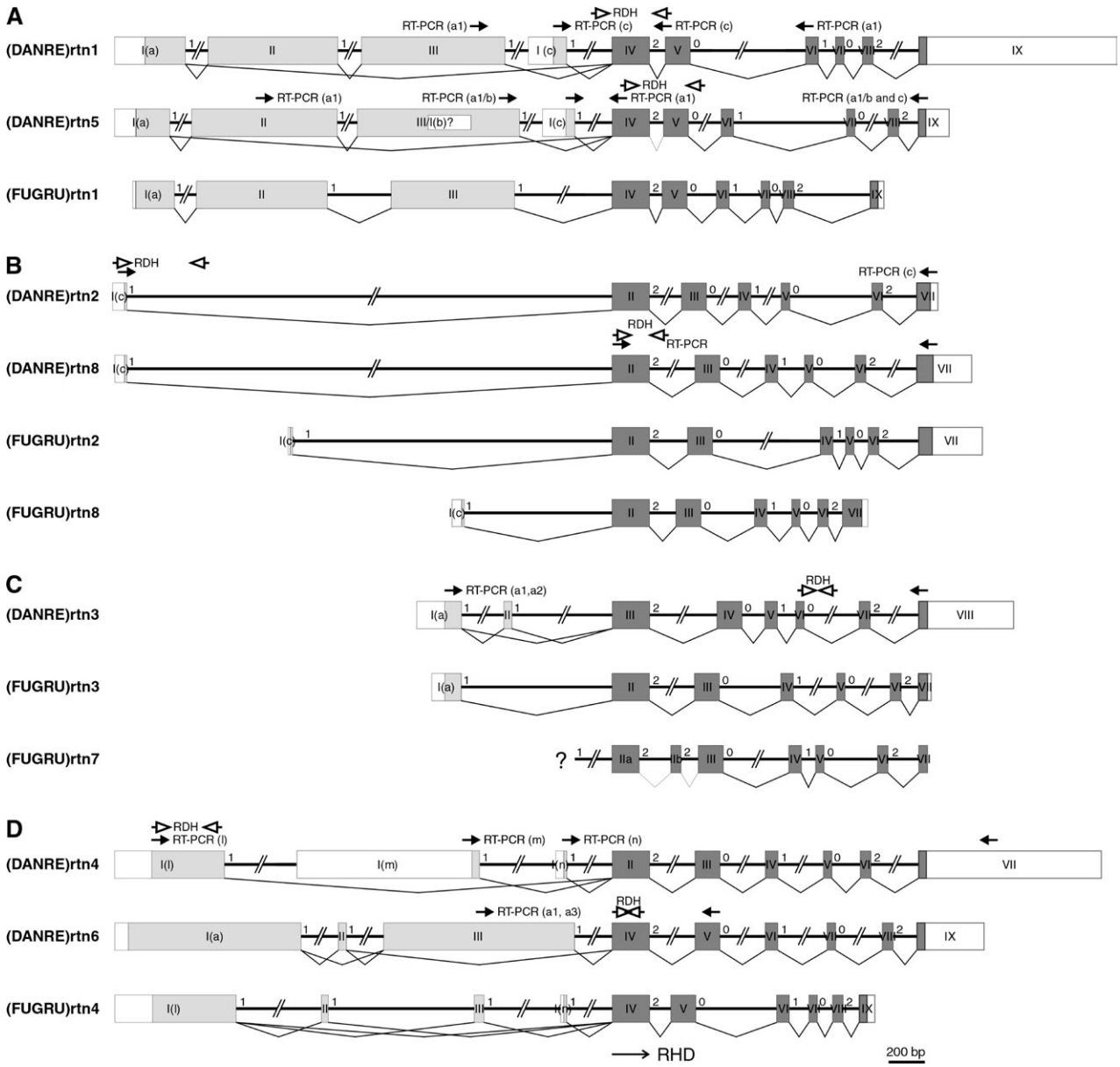

FIG. 4. Analysis of zebrafish and pufferfish *rtn* genes. Exon intron arrangements are schematically shown. Exons are drawn as roman numbered boxes. The coding regions for paralog specific amino termini are shaded light gray and exons of the RHDs are shaded dark gray. UTRs are depicted as open boxes. Intron phases are specified with arabic numerals. Localizations of primers used for analyses of the zebrafish genes/transcripts are indicated by closed (RT PCR) and open (radiation hybrid mapping) arrows, respectively. (*A*) Exon intron arrangements of (DANRE)rtn1, (DANRE)rtn5, and (FUGRU)rtn1 genes in comparison to (Human)RTN1. (*B*) Exon intron arrangements of (DANRE)rtn8, (FUGRU)rtn2, and (FUGRU)rtn8 genes in com parison to (Human)RTN2. Human exons 1A, 2, 3, 4, and 5 (Oertle et al. 2003*b*) have been omitted from this scheme for simplicity. (*C*) Exon intron arrangements of (DANRE)rtn3, (FUGRU)rtn3, and (FUGRU)rtn7 genes in comparison to (Human)RTN3. For fugu (FUGRU)rtn7, the specific N terminal exon could not be identified within the genomic sequences (marked with ?). (*D*) Exon intron arrangements of (DANRE)rtn4, (DANRE)rtn6, and (FUGRU)rtn4 genes in comparison to (Human)RTN4. Human exons 1D, 1E, 1F, and 1G (Oertle et al. 2003*b*) have been omitted for simplicity.

of 2-0-1-0-2, while the amino-terminal exons are all symmetrical 1-1 exons (fig. 4, supplementary table 2).

In contrast, the N-terminal sequences of *rtn1 rtn8* are less conserved compared to the RHD and show no homology between the tetralogs (rtn1/5 to rtn2/8 to rtn3/7 to rtn4/6). However, the fish N-termini of rtn1/5-a, rtn1/5-c, rtn2/8-c, rtn3/7-a1, and rtn3/7-a2 are each orthologous to their mammalian counterparts. First of all, the exon-intron arrangements for the aforementioned transcripts are comparable to those of the respective mammalian isoforms (fig. 4*A C*; Oertle et al. 2003*b*). For example, both N-termini of (DANRE)rtn1-a1 and (Human)RTN1-A consist of three exons each, with similar size. The same holds true for rtn3-a2, in which particularly exon 2 is conserved (fig. 4*C*, ALIGN 000756). Secondly, although the N-terminal sequences have diverged between different species, at least stretches of conserved aa can be identified, demonstrating a common predecessor of these N-termini (ALIGN 000753, ALIGN 000754, ALIGN 000755, ALIGN 000756).

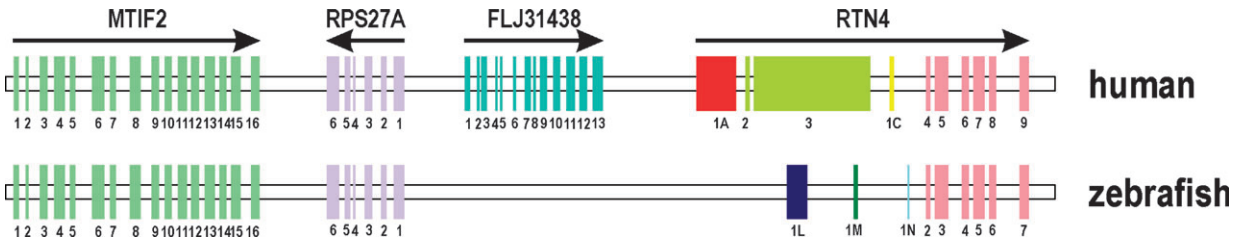

FIG. 5. Schematic comparison of the human and zebrafish *rtn4* gene locus. Scheme of the pairwise comparison between the human zebrafish RTN4 gene locus based on an ungapped alignment from the MTIF2 gene to RTN4 (supplementary fig. 3). Human *RTN4* exons are numbered according to Oertle et al. (2003*a*). Note that the *MTIF2* gene and the exons coding for the conserved C terminal RHD (exons 4 9) are conserved in human and the orthologous fish locus. In contrast, no homology of the human RTN4 exons 1A, 2, and 3 could be identified in zebrafish, unequivocally proving the absence of sequences orthologous to the N termini of mammalian RTN4 isoforms in zebrafish.

Interestingly, the N-termini of mammalian RTN4 and fish rtn4/6 show no indication for a common ancestor. Stretches of conserved aa could neither be identified between the two fish paralogs (rtn4, rtn6) nor be identified between either of the fish duplicates (rtn4/6) and mammalian RTN4 (ALIGN 000757, ALIGN 000758). Moreover, the exon-intron arrangement of the fish *rtn4* gene markedly differs from mammalian RTN4. Three alternative N-termini (-l, -m, -n) are generated by the use of three different promoters and are each encoded by a single specific exon, whereas the N-termini of mammalian RTN4 (-A, -B, -C, -D, -E, -F, -G) are represented by one to three exons (fig. 4*D*; Oertle et al. 2003*a*).

Taken together, the N-terminal parts of the rtns show higher divergence compared to the RHD, demonstrating nonhomogeneous evolution of the RTN family genes. Although not all rtn splice forms present in mammals were found in fish, detailed genomic and sequence analyses indicate that the specific N-termini of fish and mammalian rtn1/5, rtn2/8, and rtn3/7, respectively, evolved from a common ancestor. In contrast, the rtn4/6 N-termini are completely different and must have been acquired independently. Stretches of aa comparable to the mammalian neurite growth inhibitory region NiG-Δ20 were neither found in the three alternative N-termini of zebrafish rtn4 (-l, -m, and -n) nor found in rtn6-a1.

Absence of Exons Homologous to Mammalian Nogo-A

To unequivocally exclude the presence of exons homologous to the N-terminal region of mammalian Nogo-A in zebrafish, we compared the genomic region of (DANRE)*rtn4* against the orthologous human and mouse genomic regions using an ungapped alignment of zebrafish versus mammalian genomic sequences ranging from the nearest common gene lying 5′ to RTN4 on the same coding strand to the six exons encoding the RHD (fig. 5, supplementary fig. 3). We identified *MTIF*2 (Bonner, Wiley, and Farwell 1998) as the nearest gene lying 5′ to *rtn4* on the same coding strand in zebrafish, mouse, and human. The two human genes *FLJ31438* and *RPS27A* are in fact located closer to *rtn4*, but an orthologous *FLJ31438* gene is not present in zebrafish, and *RPS27A* is encoded by the complementary strand. As shown in the PIP (supplementary fig. 3*A* and *B*), the coding exons of the *MTIF2* gene and the six exons of the rtn4 RHD are well conserved in both mammals and zebrafish. However, within the genomic region 5′ of the RHD, no stretches homologous to the N-terminal exons of mammalian Nogo-A (human RTN4 exons 1A, 2, 3, and 1C G) could be identified in zebrafish (fig. 5, supplementary fig. 3). Consequently, the ungapped alignment from the *MTIF2* gene to *RTN4* unequivocally proved the absence of exons homologous to any known human isoforms in zebrafish.

In addition, Blast searches with the sequence encoding the N-terminal region of human Nogo-A did not reveal any significant homology (>20% identity) to any other (non-rtn) zebrafish gene (data not shown). Thus, the neurite outgrowth inhibitory region in the N-terminus of Nogo-A (NiG-Δ20; Oertle et al. 2003*c*) is not present in zebrafish.

RT-PCR Analyses of Zebrafish rtn Expression

The finding that rtn4 transcripts with functions similar to mammalian Nogo-A are absent in zebrafish would be substantiated by the verification of dissimilar expression patterns of fish rtn4-l, -m, and -n in comparison to mammalian RTN4-A/Nogo-A. In addition, transcription of the other fish rtn mRNAs during zebrafish development and in different adult tissues was analyzed (fig. 6A L) not only to characterize each rtn splice form but also to compare the expression of recently duplicated gene paralogs (e.g., rtn4 rtn6) and to obtain information about potential subfunctionalizations. The observed temporal expression patterns of the rtns can be assigned to three distinct groups. In zebrafish embryos and larvae (fig. 6, right panel), many rtn cDNAs are ubiquitously expressed without temporal variations (rtn1-a1, rtn5-b, rtn5-c, rtn3-a1, rtn4-l, and rtn4-n). Four transcripts show no (rtn5-a1, rtn2-c) or less (rtn4-m, rtn6-a1) expression at early developmental stages, whereas quite dynamic patterns are observed for rtn1-c and rtn8. All transcripts that are omnipresent during zebrafish development are also ubiquitously expressed in various adult tissues (rtn1-a1, rtn5-b, rtn5-c, rtn3-a1, and rtn4-l) with the exception that rtn1-a1 and rtn5-c are hardly detectable in gills (fig. 6, left panel). Rtn4-n and rtn6-a1 transcripts were found in all tissues analyzed, but to a varying degree. Six of the analyzed zebrafish rtn transcripts show rather tissue-specific expression (rtn1-c, rtn5-a1, rtn2-c, rtn8, rtn3-a2, and rtn4-m).

Overall, the extensive RT-PCR analyses revealed differences in the spatial and/or temporal expression patterns of corresponding paralogous transcripts (rtn1-a1/5-a1; rtn1-c/5-c). For example, onset of rtn5-a1 transcription is

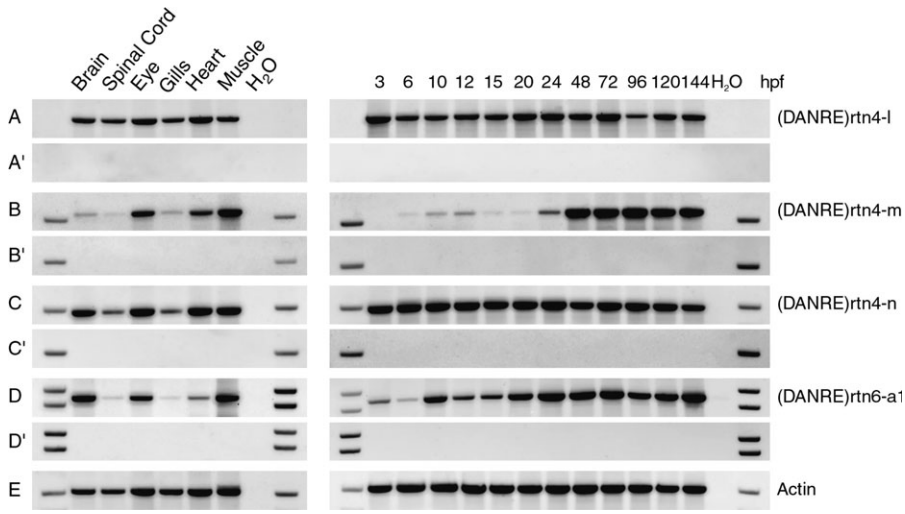

FIG. 6. RT PCR analyses of zebrafish rtn mRNA expression. Expression of zebrafish rtn mRNAs was examined by RT PCR (A L). A reverse transcriptase negative control (without Superscript II enzyme) was performed with each primer pair (A′ L′). RT PCR with actin specific primers (Actin) served as a positive control and to ensure that equal amounts of cDNA template were put into each reaction (M). During development (3 144 hpf, right panel), rtn1 a1, rtn5 b, rtn5 c, rtn3 a1, rtn4 l, and rtn4 n are ubiquitously expressed (A, I, J, D, E, and G, respectively). Rtn5 a1, rtn2 c, rtn4 m, and rtn6 a1 show less expression at early developmental stages (H, C, F, and K, respectively). Rtn1 c expression is quite dynamic with repeatedly low mRNA levels at 3 and 15 hpf (B). The level of rtn8 mRNA is significantly decreased between 6 and 20 hpf (L). Note that the rtn8 RT PCR detects the RHD and is not specific for a single isoform, but only rtn8 c is known so far. In the adult tissues analyzed (left panel), rtn1 a1, rtn5 b, rtn5 c, rtn3 a1, rtn4 l, rtn4 n, and rtn6 a1 are omnipresent, but some show varying expression levels (A, I, J, D, E, G, and K, respectively). Rtn1 c, rtn5 a1, rtn2 c, rtn8, rtn3 a2, and rtn4 m are rather tissue specifically expressed (B, H, C, L, D, and F, respectively). Note that rtn5 RT PCRs with a sense primer located either in exon II or at the 3′ end of exon III (fig. 1*A*) give totally different patterns (H, I). We therefore propose the existence of a third alternative promoter giving rise to a transcript that we call rtn5 b (fig. 1*A*). Abbreviations: hpf, hours postfertilization; H_2O, no template control.

delayed with respect to rtn1-a1, meaning that only rtn1-a1 is present at early developmental stages. High-level rtn5-c in contrast to low rtn1-c expression in muscle and heart reveals tissue-specific discrimination. Because the structure of the paralogous *rtn4* and *rtn6* genes differ for the N-terminal exons (three alternative promoters for rtn4 compared to one promoter but alternative splicing of three exons for rtn6; fig. 4*D*), the resulting transcripts are not orthologous and therefore not directly comparable. Nevertheless, the expression patterns of rtn4-l, -m, or -n are not similar to rtn6-a1. These divergences in the expression of duplicated genes indicate a potential subfunctionalization. We therefore conclude that none of the gene copies is redundant and that, in particular, the paralogous rtn4 and rtn6 proteins exert different functions in fish. Moreover, none of the patterns of the four fish rtn4-homologous transcripts (rtn4-l, -m, -n and rtn6-a1) fits to the expression of the axon growth inhibitory mammalian RTN4-A/Nogo-A in neurons and oligodendrocytes (Oertle and Schwab 2003), although both mammal and fish rtn4 isoforms are expressed widely and early in development. This provides additional evidence that the identified fish rtn4 transcripts do not exert neurite growth inhibitory functions similar to mammalian Nogo-A.

Discussion

The *rtn* gene family member Nogo-A/RTN4-A has been widely described as a potent inhibitor of axon regeneration in mammals (Chen et al. 2000; GrandPré et al. 2000; Prinjha et al. 2000; Brittis and Flanagan 2001). In the fish CNS, however, lesioned axons readily regenerate, and fish CNS myelin has been proven to be a permissive substrate for the growth of axons (Bastmeyer et al. 1991; Wanner et al. 1995). Interestingly, fish axons are nevertheless repelled by rat oligodendrocytes in vitro. Here, we showed that growth inhibition of fish retinal axons is mediated by the inhibitory activity of the Nogo-A specific peptide NiG-Δ20. Together with earlier findings (Bastmeyer et al. 1991; Wanner et al. 1995), this result led to the speculation that Nogo-A may not be present in the fish CNS.

Because *rtn4*/*nogo* is a member of a large gene family with the highly conserved C-terminal RHD (Oertle et al. 2003*b*), phylogenetic analyses of all vertebrate *rtn* members coupled with gene mapping and synteny data were necessary for the correct assignment of a true fish *rtn4* ortholog. We therefore cloned seven zebrafish and five pufferfish *rtn* genes and uncovered 30 additional *rtn* genes in eight different fish species by database searches. Our phylogenetic analyses based on the conserved RHD indicate that the four subgroups of the vertebrate RTN family (RTN1 4) arose by duplication events before the divergence of tetrapods (sarcopterygians) and ray-finned fish (actinopterygians) and that we identified at least one zebrafish and fugu ortholog for each subgroup. The presence of additional genes for each of the tetralogs *rtn1 4* either in zebrafish and/or pufferfish that can also be seen in other fish species (e.g., carp *rtn1/5* and carp *rtn4/6*) is consistent with the prediction of the fish-specific genome duplication hypothesis (Amores et al. 1998; Taylor et al. 2003). The phylogenetic relationships of the *rtn* genes identified in Salmonidae, however, cannot solely be explained by this 2R hypothesis. An additional genome duplication leading to possibly 16 different *rtn* genes (fig. 7) has to be proposed in this fish subgroup

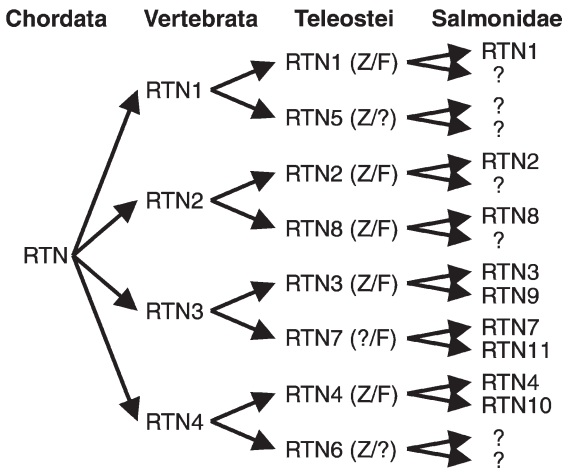

FIG. 7. Schematic overview of duplicated fish rtn genes. A single *rtn* gene is present in the urochordate *Ciona intestinalis*. The divergence of the *rtn* family in fish was produced by separate duplication events in the an cestors of vertebrates and early in actinopterygian evolution, leading to rtn1 to rtn8 in teleostei. For Salmonidae, an additional genome duplication has to be postulated. Abbreviations: Z, the respective *rtn* gene has been identified in zebrafish; F, the respective *rtn* gene has been identified in fugu; ?, the respective *rtn* gene has yet to be identified or has specifically been lost.

(Brunelli, Robison, and Thorgaard 2001; Rise et al. 2004). Assuming the validity of the genome duplications early in actinopterygian evolution and in Salmonidae, it has to be postulated that several zebrafish, fugu, and salmon *rtn* genes have yet to be discovered or specific gene losses have occurred (fig. 7). The differences in gene expression of duplicated *rtn* genes and in some cases the rapid sequence divergence of duplicated genes potentially generating alternative functional properties (e.g., relatively low sequence homology of *rtn4* and *rtn6*) could explain why highly related paralogs were maintained in the fish genomes instead of rapidly mutating to pseudogenes (Meyer and Schartl 1999).

The identity of the zebrafish *rtn* orthologs was confirmed by radiation hybrid mapping and synteny analyses. All seven zebrafish *rtn* genes are positioned within syntenic gene clusters, i.e., genes in the vicinity of a given *rtn* are the same on the zebrafish and the respective human chromosomes. Similar results were obtained for three of the six fugu genes. Moreover, our phylogenetic result of duplication of *rtn1 4* in fish is substantiated by the synteny data that zebrafish paralogs map to regions syntenic with the same human chromosome, e.g., zebrafish *rtn1* and *rtn5* both with human Chr. 14. Although *rtn5* and *rtn6* both map to the same zebrafish chromosome (LG13), it is unlikely that these genes are the result of a tandem duplication. The distance between *rtn5* and *rtn6* is rather large, and each gene is located in a region that is syntenic to a different human chromosome (Chr. 14 and Chr. 2, respectively). Taken together, our detailed phylogenetic and syntenic analyses clearly demonstrate that a true fish ortholog of the mammalian *rtn4*/*nogo* gene exists and that the fish gene has been duplicated, leading to the two paralogs *rtn4* and *rtn6*. Due to the increased accumulation of aa-altering substitutions, *rtn6* is yet more distantly related to human RTN4.

To obtain indications whether the fish orthologs would exert a similar axon growth inhibitory function as the mammalian Nogo-A protein, we dissected the N-termini of fish rtn4 and rtn6 for the presence of homologous aa stretches that have been shown to exert the inhibitory function of mammalian Nogo-A (i.e., NiG-Δ20) and compared their evolution with the evolution of the rtn1 3 N-termini. The N-termini of all *rtn* genes are far more divergent than their RHDs; still for rtn1/5, rtn2/8, and rtn3/7, the genomic structures of the fish and the respective mammalian genes are comparable and stretches of conserved aa are detectable within these N-termini. Consequently, the N-termini of fish and mammalian rtn1 3 isoforms are orthologous and derived from a common ancestor. These findings are comparable with the nonhomogenous evolution of different parts of the annexin proteins, which has also led to evolutionary conserved C-termini and highly variable N-termini. The annexin N-termini show recognizable homology only in functionally important domains, e.g., phosphorylation sites (Farber et al. 2003). The various alternative fish and mammalian rtn4/6 N-termini, in contrast to rtn1 3, have conserved neither genomic organizations nor stretches of similar aa, which argues against a common ancestor of fish and mammalian rtn4/6 N-termini. Moreover, examination of the genomic region upstream of the zebrafish *rtn4* gene proves the absence of exons homologous to the mammalian RTN4-A/B specific exons 1A, 2, and 3 (Oertle et al. 2003*a*). Thus, the N-termini of fish and mammalian rtn4 have a different evolutionary origin, and the neurite outgrowth inhibitory region NiG-Δ20 of mammalian Nogo-A (rat aa 544 575) is not present in zebrafish. This result correlates with the acquisition of Nogo-A specific sequences and the concurrent loss of the ability for axon regeneration during the transition from fish to land vertebrates (Stuermer et al. 1992). In comparison, myelin-associated glycoprotein and oligodendrocyte myelin glycoprotein, two other molecules identified as mammalian CNS inhibitors, are present in zebrafish (Lehmann et al. 2004; data not shown). This suggests that the absence of Nogo-A is causally related to successful axonal regeneration in fish. On the other hand, yet unidentified functions not related to axonal growth inhibition are expected for fish rtn4. Owing to the fact that orthologous N-termini for mammalian Nogo-A have been identified in amphibian and avian organisms (Oertle et al. 2003*b*; Klinger et al. 2004*a*), future studies will have to concentrate on the evolutionary origin of this region in organisms linking the transition between fish and amphibians.

The sequence of the second potential growth inhibitory domain, Nogo-66, which is located in the C-terminal RHD of all RTN4/Nogo isoforms, is present in fish, and the conservation throughout the whole RHD is rather high. No changes in key residues or differing domains within either the tetrapods or the fish rtn4/6 RHD could be identified that could explain the growth inhibitory function of Nogo-66 on one side (tetrapods) and the lack of inhibition on the other (fish). Still, several results and considerations argue against an inhibitory influence of fish Nogo-66. The widespread expression of all zebrafish rtn4/6 transcripts including a variety of nonneuronal tissues rather contradicts an axon growth inhibitory function. Because rtn4 transcripts are also

present in goldfish oligodendrocytes (M. Klinger, unpublished data) and fish express the corresponding receptor NgR (Klinger et al. 2004*b*), a functional receptor-ligand interaction is conceivable. In contrast to mammals (Fournier, GrandPré, and Strittmatter 2001; GrandPré, Li, and Strittmatter 2002), however, this interaction obviously does not lead to the inhibition of axon growth in fish because fish axons grow over isolated fish oligodendrocytes in vitro (Bastmeyer et al. 1991; Stuermer et al. 1992) and readily regenerate in vivo (Stuermer et al. 1992). Therefore, if Nogo-66 interacts with NgR in fish, this interaction is coupled to an intracellular signaling cascade different from that in mammals. Alternatively, the homologous fish Nogo-66 region might not be exposed to the extracellular surface of fish oligodendrocytes and therefore not be accessible for an interaction with NgR. Future studies will show if a molecular interaction between fish Nogo-66 and NgR mediates any inhibitory activity or serves totally different purposes. This could shed light on the physiological importance of Nogo-66 as an inhibitor of axonal regeneration also in mammals.

In summary, evolution of the fish *rtn4/6* genes has combined exons encoding the RHD with exons entirely different from mammalian and amphibian Nogo-A, -B, and -C encoding exons. Sequences related to the Nogo-A major inhibitory domain NiG-Δ20 are absent from fish. While this is congruent with the growth permissiveness of fish CNS myelin, the question why fish axons respond to mammalian Nogo-A remains to be addressed in future studies.

Supplementary Material

The following supplementary materials are available at *Molecular Biology and Evolution* online (http://www.mbe.oxfordjournals.org/):

SUPPLEMENTARY FIG. 1. Diagnostic residues for vertebrate RTN subfamilies. The nine residues conserved (monomorphic) in all vertebrates RTN1 RTN4 sequences and *Ciona* RTN are shaded in gray and marked by an arrow above the alignment. Residues unique to one RTN subfamily (RTN1, 2, 3, or 4) are highlighted in red. Residues within each RTN1 RTN4 subfamily that are unique to either land vertebrate or fish proteins are highlighted in blue. All residues conserved with the respective *Ciona* residue (ancestral) are represented by dots. Sequences that did not comprise the full RHD received the suffix "w." The 66-aa loop between the two transmembrane regions of the RHD is denoted above the alignment (Nogo-66). Abbreviations: BOVIN, *Bos taurus*; CANFA, *Canis familiaris*; CARAU, *Carassius auratus*; CHICK, *Gallus gallus*; CIOIN, *Ciona intestinalis*; CYPCA, *Cyprinus carpio*; DANRE, *Danio rerio*; FUGRU, *Takifugu rubripres*; GASAC, *Gasterosteus aculeatus*; ICTPU, *Ictalurus punctatus*; HUMAN, *Homo sapiens*; MACMU, *Macaca mulatta*; MACFA, *Macaca fascicularis*; MOUSE, *Mus musculus*; ONCMY, *Oncorhynchus mykiss*; ORYLA, *Oryzias latipes*; PANTR, *Pan troglodytes*; PAROL, *Paralichthys olivaceus*; PIG, *Sus scrofa*; RAT, *Rattus norvegicus*; SHEEP, *Ovis aries*; SALSA, *Salmo salar*; XENLA, *Xenopus laevis*; XENTR, *Silurana tropicalis*.

SUPPLEMENTARY FIG. 2. Cryptic splice variants of (DANRE)rtn4, rtn5, and rtn6. Schematic drawing of mRNA variants that result from internal splicing at cryptic donor and acceptor sites. (*A*) Two minor rtn4-l spliceforms due to internal splicing of the first exon were amplified from cDNA. The start codon of these transcripts would shift to a new position. (*B*) Internal splicing in exons II and III of rtn6-a1 leads to either internal, in-frame deletions or premature stops (*). (*C*) Internal splicing in exons II, III, and IV of rtn5-a1.

SUPPLEMENTARY FIG. 3. PIP of the human, mouse, and zebrafish rtn4 gene locus. Graphical representation of pairwise comparisons between the human-mouse (mouse) and human-zebrafish (danre) *MTIF2* to *rtn4* gene locus using a PIP in which the percent identity (from 50% to 100%) in each gap-free aligning segment is plotted using the coordinates of the human sequence. The entire alignment is represented by three consecutive parts (*A*, *B*, and *C*). The human RTN4 exons (*C*) are numbered according to Oertle et al. (2003*a*), while the exons of human *MTIF2* (*A*), *RPS27A* (*A*), and *FLJ31438* (*A*, *B*) have been consecutively numbered from 5′ to 3′. The *MTIF2* gene region is shown in green, *RPS27A* (encoded on the reverse strand) in purple, *FLJ31438* in blue, and *RTN4* (*C*) in red. Exons are marked in darker color. Coding exons are shown as black boxes above the alignment, while untranslated exonic regions are depicted as gray boxes. Almost all coding exons of *MTIF2* and *RPS27A* are strongly conserved in human, mouse, and zebrafish (*A*). The *FLJ31438* gene (*A*, *B*), however, is present in human and mouse but absent in zebrafish, suggesting that this gene has been acquired at a later evolutionary stage in vertebrate phylogeny. Almost the entire genomic region between *RPS27A* and exon 4 of *RTN4* shows no or very low homologies in zebrafish (*A C*). Note that while the N-terminal exons 1A, 2, and 3 are strongly conserved in the murine orthologous region, no homology could be identified in zebrafish. In contrast, the exons coding for the conserved C-terminal RHD (exons 4 9) are also conserved in the fish orthologous locus. The ungapped alignment from the *MTIF2* gene to *RTN4* is unequivocally proving the absence of sequences orthologous to the N-termini of mammalian RTN4 isoforms in zebrafish. For the analysis and explanation of the interspersed repetitive elements please refer to the PIP in Oertle et al. (2003*a*).

Supplementary Table 1A: Overview of cloned zebrafish and fugu rtns.

Supplementary Table 1B: Primer used for RT-PCR and radiation hybrid mapping.

Supplementary Table 1C: RT-PCR conditions.

Supplementary Table 1D: GenBank accession numbers of vertebrate rtn genes.

Supplementary Table 1E: Rates of nonsynonymous substitutions per nonsynonymous site (d_N) and rates of synonymous substitutions per synonymous site (d_S) calculated for the RHD.

Supplementary Table 1F K: Mapping data for the analyses of conserved syntenies between zebrafish and human, with respect to rtns.

Supplementary Table 1L: Mapping data for the analyses of conserved syntenies between fugu and human, with respect to rtns.

Supplementary Table 2: Exon and intron sizes of zebrafish and fugu rtns.

Sequence alignments deposited at EMBL-ALIGN (http://www.ebi.ac.uk/embl/Submission/align top.html):

ALIGN 000759: BioEdit alignment of RHD sequences,
ALIGN 000753: BioEdit alignment of rtn1-a/5-a N-termini,
ALIGN 000754: BioEdit alignment of rtn1-c/5-c N-termini,
ALIGN 000755: BioEdit alignment of rtn2-c/8-c N-termini,
ALIGN 000756: BioEdit alignment of rtn3-a/7-a N-termini,
ALIGN 000757: BioEdit alignment of mammalian rtn4-a and fish rtn4-l/6-a N-termini,
ALIGN 000758: BioEdit alignment of mammalian rtn4-c and fish rtn4-n N-termini.

Acknowledgments

This work was supported by grants of the Deutsche Forschungsgemeinschaft (DFG) and of the Fonds der Chemischen Industrie to C.A.O.S. M.K. was supported by the Stiftung der Deutschen Wirtschaft für Qualifizierung und Kooperation e.V. and H.-M.P. by the DFG (DFG PO807/1-1). We thank M.-A. Cahill for technical assistance, C. Haenisch for her help in the RT-PCR analysis, A. Y. Loos for fish care, and J. S. Taylor for critical reading of the manuscript.

Literature Cited

Altschul, S. F., T. L. Madden, A. A. Schaffer, J. Zhang, Z. Zhang, W. Miller, and D. J. Lipman. 1997. Gapped BLAST and PSI BLAST: a new generation of protein database search programs. Nucleic Acids Res. **25**:3389 3402.

Amores, A., et al. (13 co authors). 1998. Zebrafish hox clusters and vertebrate genome evolution. Science **282**:1711 1714.

Baka, I. D., N. N. Ninkina, L. G. Pinon, J. Adu, A. M. Davies, G. P. Georgiev, and V. L. Buchman. 1996. Intracellular com partmentalization of two differentially spliced s rex/NSP mRNAs in neurons. Mol. Cell. Neurosci. **7**:289 303.

Barbazuk, W. B., I. Korf, C. Kadavi, J. Heyen, S. Tate, E. Wun, J. A. Bedell, J. D. McPherson, and S. L. Johnson. 2000. The syn tenic relationship of the zebrafish and human genomes. Genome Res. **10**:1351 1358.

Bastmeyer, M., M. Beckmann, M. E. Schwab, and C. A. Stuermer. 1991. Growth of regenerating goldfish axons is inhibited by rat oligodendrocytes and CNS myelin but not by goldfish optic nerve tract oligodendrocyte like cells and fish CNS myelin. J. Neurosci. **11**:626 40.

Bonner, D. S., J. E. Wiley, and M. A. Farwell. 1998. Assignment1 of the mitochondrial translational initiation factor 2 gene (MTIF2) to human chromosome 2 bands p16→p14 by in situ hybridization and with somatic cell hybrids. Cytogenet. Cell Genet. **83**:80 81.

Brittis, P. A., and J. G. Flanagan. 2001. Nogo domains and a Nogo receptor: implications for axon regeneration. Neuron **30**: 11 14.

Brunelli, J. P., B. D. Robison, and G. H. Thorgaard. 2001. Ancient and recent duplications of the rainbow trout Wilms' tumor gene. Genome **44**:455 462.

Chen, M. S., A. B. Huber, M. E. van der Haar, M. Frank, L. Schnell, A. A. Spillmann, F. Christ, and M. E. Schwab. 2000. Nogo A is a myelin associated neurite outgrowth inhib itor and an antigen for monoclonal antibody IN 1. Nature **403**:434 439.

Farber, S. A., R. A. De Rose, E. S. Olson, and M. E. Halpern. 2003. The zebrafish annexin gene family. Genome Res. **13**:1082 1096.

Felsenstein, J. 1985. Confidence limits on phylogenies: an ap proach using the bootstrap. Evolution **39**:783 791.

Filbin, M. T. 2003. Myelin associated inhibitors of axonal regen eration in the adult mammalian CNS. Nat. Rev. Neurosci. **4**:703 713.

Fournier, A. E., T. GrandPré, and S. M. Strittmatter. 2001. Identification of a receptor mediating Nogo 66 inhibition of axonal regeneration. Nature **409**:341 346.

Gaze, R. M. 1970. The formation of nerve connections. Academic Press Inc., New York.

Geisler, J. G., L. J. Stubbs, W. W. Wasserman, and M. L. Mucenski. 1998. Molecular cloning of a novel mouse gene with predominant muscle and neural expression. Mamm. Genome **9**:274 282.

GrandPré, T., S. Li, and S. M. Strittmatter. 2002. Nogo 66 recep tor antagonist peptide promotes axonal regeneration. Nature **417**:547 551.

GrandPré, T., F. Nakamura, T. Vartanian, and S. M. Strittmatter. 2000. Identification of the Nogo inhibitor of axon regeneration as a reticulon protein. Nature **403**:439 444.

Hall, T. A. 1999. BioEdit: a user friendly biological sequence alignment editor and analysis program for Windows 95/98/ NT. Nucleic Acids Symp. Ser. **41**:95 98.

Hamada, N., J. Iwahashi, K. Suzuki, H. Ogi, T. Kashiwagi, K. Hara, M. Toyoda, T. Yamada, and T. Toyoda. 2002. Molecular cloning and characterization of the mouse reticulon 3 cDNA. Cell. Mol. Biol. (Noisy le grand) **48**:163 172.

Hukriede, N. A., et al. (17 co authors). 1999. Radiation hybrid mapping of the zebrafish genome. Proc. Natl. Acad. Sci. USA **96**:9745 9750.

Klinger, M., H. Diekmann, D. Heinz, C. Hirsch, S. Hannbeck von Hanwehr, B. Petrausch, T. Oertle, M. E. Schwab, and C. A. O. Stuermer. 2004*a*. Identification of two nogo/rtn4 genes and analysis of Nogo A expression in Xenopus laevis. Mol. Cell. Neurosci. **25**:205 216.

Klinger, M., J. S. Taylor, T. Oertle, M. E. Schwab, C. A. Stuermer, and H. Diekmann. 2004*b*. Identification of Nogo 66 receptor (NgR) and homologous genes in fish. Mol. Biol. Evol. **21**: 76 85.

Kools, P. F., A. J. Roebroek, H. J. Van de Velde, P. Marynen, J. Bullerdiek, and W. J. Van de Ven. 1994. Regional mapping of the human NSP gene to chromosome region 14q21→q22 by fluorescence in situ hybridization analysis. Cytogenet. Cell Genet. **66**:48 50.

Kozak, M. 1996. Interpreting cDNA sequences: some insights from studies on translation. Mamm. Genome **7**:563 574.

Kumar, S., K. Tamura, I. B. Jakobsen, and M. Nei. 2001. MEGA2: molecular evolutionary genetics analysis software. Bioinformatics **17**:1244 1245.

Lehmann, F., H. Gathje, S. Kelm, and F. Dietz. 2004. Evolution of sialic acid binding proteins: molecular cloning and expression of fish siglec 4. Glycobiology **14**:959 968.

Mayor, C., M. Brudno, J. R. Schwartz, A. Poliakov, E. M. Rubin, K. A. Frazer, L. S. Pachter, and I. Dubchak. 2000. VISTA: visualizing global DNA sequence alignments of arbitrary length. Bioinformatics **16**:1046 1047.

Meyer, A., and M. Schartl. 1999. Gene and genome duplications in vertebrates: the one to four (to eight in fish) rule and the

evolution of novel gene functions. Curr. Opin. Cell Biol. **11**:699 704.

Moreira, E. F., C. J. Jaworski, and I. R. Rodriguez. 1999. Cloning of a novel member of the reticulon gene family (RTN3): gene structure and chromosomal localization to 11q13. Genomics **58**:73 81.

Morris, N. J., S. A. Ross, J. M. Neveu, W. S. Lane, and G. E. Lienhard. 1999. Cloning and characterization of a 22 kDa pro tein from rat adipocytes: a new member of the reticulon family. Biochim. Biophys. Acta **1450**:68 76.

Nagase, T., K. Ishikawa, N. Miyajima, A. Tanaka, H. Kotani, N. Nomura, and O. Ohara. 1998. Prediction of the coding sequences of unidentified human genes. IX. The complete sequences of 100 new cDNA clones from brain which can code for large proteins in vitro. DNA Res. **5**:31 39.

Nei, M., and T. Gojobori. 1986. Simple methods for estimating the numbers of synonymous and nonsynonymous nucleotide sub stitutions. Mol. Biol. Evol. **3**:418 426.

Ninkina, N. N., I. D. Baka, and V. L. Buchman. 1997. Rat and chicken s rex/NSP mRNA: nucleotide sequence of main transcripts and expression of splice variants in rat tissues. Gene **184**:205 210.

Oertle, T., C. Huber, H. van der Putten, and M. E. Schwab. 2003*a*. Genomic structure and functional characterisation of the pro moters of human and mouse nogo/rtn4. J. Mol. Biol. **325**: 299 323.

Oertle, T., M. Klinger, C. A. Stuermer, and M. E. Schwab. 2003*b*. A reticular rhapsody: phylogenic evolution and nomenclature of the RTN/Nogo gene family. FASEB J. **17**:1238 1247.

Oertle, T., D. Merkler, and M. E. Schwab. 2003. Do cancer cells die because of Nogo B? Oncogene **22**:1390 1399.

Oertle, T., and M. E. Schwab. 2003. Nogo and its paRTNers. Trends Cell Biol. **13**:187 194.

Oertle, T., et al. (13 co authors). 2003*c*. Nogo A inhibits neurite outgrowth and cell spreading with three discrete re gions. J. Neurosci. **23**:5393 5406.

Prinjha, R., S. E. Moore, M. Vinson, S. Blake, R. Morrow, G. Christie, D. Michalovich, D. L. Simmons, and F. S. Walsh. 2000. Inhibitor of neurite outgrowth in humans. Nature **403**:383 384.

Rise, M. L., et al. (29 co authors). 2004. Development and appli cation of a salmonid EST database and cDNA microarray: data mining and interspecific hybridization characteristics. Genome Res. **14**:478 490.

Roebroek, A. J., T. A. Ayoubi, H. J. Van de Velde, E. F. Schoenmakers, I. G. Pauli, and W. J. Van de Ven. 1996. Genomic organization of the human NSP gene, prototype of a novel gene family encoding reticulons. Genomics **32**:191 199.

Roebroek, A. J., B. Contreras, I. G. Pauli, and W. J. Van de Ven. 1998. cDNA cloning, genomic organization, and expression of the human RTN2 gene, a member of a gene family encoding reticulons. Genomics **51**:98 106.

Roebroek, A. J., H. J. van de Velde, A. Van Bokhoven, J. L. Broers, F. C. Ramaekers, and W. J. Van de Ven. 1993. Cloning and expression of alternative transcripts of a novel neuroendocrine specific gene and identification of its 135 kDa translational product. J. Biol. Chem. **268**:13439 13447.

Schwab, M. E. 2004. Nogo and axon regeneration. Curr. Opin. Neurobiol. **14**:118 124.

Schwartz, S., Z. Zhang, K. A. Frazer, A. Smit, C. Riemer, J. Bouck, R. Gibbs, R. Hardison, and W. Miller. 2000. PipMaker a web server for aligning two genomic DNA sequences. Genome Res. **10**:577 586.

Stubbs, L., et al. (12 co authors). 1996. Detailed comparative map of human chromosome 19q and related regions of the mouse genome. Genomics **35**:499 508.

Stuermer, C. A., M. Bastmeyer, M. Bahr, G. Strobel, and K. Paschke. 1992. Trying to understand axonal regeneration in the CNS of fish. J. Neurobiol. **23**:537 550.

Stuermer, C. A. O. 1988*a*. Trajectories of regenerating retinal ax ons in the goldfish tectum: I. A comparison of normal and re generated axons at late regeneration stages. J. Comp. Neurol. **267**:55 68.

. 1988*b*. Trajectories of regenerating retinal axons in the goldfish tectum: II. Exploratory branches and growth cones on axons at early regeneration stages. J. Comp. Neurol. **267**:69 91.

Taylor, J. S., I. Braasch, T. Frickey, A. Meyer, and Y. Van De Peer. 2003. Genome duplication, a trait shared by 22,000 spe cies of ray finned fish. Genome Res. **13**:382 390.

Thompson, J. D., D. G. Higgins, and T. J. Gibson. 1994. CLUSTAL W: improving the sensitivity of progressive multiple sequence alignment through sequence weighting, position specific gap penalties and weight matrix choice. Nucleic Acids Res. **22**:4673 4680.

van de Velde, H. J., A. J. Roebroek, N. H. Senden, F. C. Ramaekers, and W. J. Van de Ven. 1994. NSP encoded retic ulons, neuroendocrine proteins of a novel gene family associ ated with membranes of the endoplasmic reticulum. J. Cell Sci. **107**:2403 2416.

Vielmetter, J., and C. A. Stuermer. 1989. Goldfish retinal axons respond to position specific properties of tectal cell membranes in vitro. Neuron **2**:1331 1339.

Wanner, M., D. M. Lang, C. E. Bandtlow, M. E. Schwab, M. Bastmeyer, and C. A. Stuermer. 1995. Reevaluation of the growth permissive substrate properties of goldfish optic nerve myelin and myelin proteins. J. Neurosci. **15**:7500 7508.

Woods, I. G., P. D. Kelly, F. Chu, P. Ngo Hazelett, Y. L. Yan, H. Huang, J. H. Postlethwait, and W. S. Talbot. 2000. A compar ative map of the zebrafish genome. Genome Res. **10**: 1903 1914.

Yang, J., L. Yu, A. D. Bi, and S. Y. Zhao. 2000. Assignment of the human reticulon 4 gene (RTN4) to chromosome 2p14→2p13 by radiation hybrid mapping. Cytogenet. Cell Genet. **88**: 101 102.

Yoder, J. A., and G. W. Litman. 2000. The zebrafish fth1, slc3a2, men1, pc, fgf3 and cycd1 genes define two regions of conserved synteny between linkage group 7 and human chromosome 11q13. Gene **261**:235 242.

Zhang, Z., P. Harrison, and M. Gerstein. 2002. Identification and analysis of over 2000 ribosomal protein pseudogenes in the human genome. Genome Res. **12**:1466 1482.

Claudia Kappen, Associate Editor